AJNR

Erdheim-Chester Disease of the Central Nervous System: New Manifestations of a Rare Disease

P. Sedrak, L. Ketonen, P. Hou, N. Guha-Thakurta, M.D. Williams, R. Kurzrock and J.M. Debnam

AJNR Am J Neuroradiol 2011, 32 (11) 2126-2131
doi: https://doi.org/10.3174/ajnr.A2707
http://www.ajnr.org/content/32/11/2126

ORIGINAL RESEARCH

P. Sedrak
L. Ketonen
P. Hou
N. Guha-Thakurta
M.D. Williams
R. Kurzrock
J.M. Debnam

Erdheim-Chester Disease of the Central Nervous System: New Manifestations of a Rare Disease

BACKGROUND AND PURPOSE: ECD is a rare non-Langerhans-cell histiocytosis, which can involve the CNS; therefore, CNS imaging findings have been described in only a small number of patients. To gain additional insight into the CNS manifestations of ECD, we reviewed the findings on imaging of the brain, head and neck, and spine in patients with ECD who presented to our institution. Here, we illustrate manifestations that have not, to our knowledge, been previously described.

MATERIALS AND METHODS: CT, MR imaging, and PET/CT studies of the brain, maxillofacial region, and spine were reviewed in 11 patients with ECD.

RESULTS: Four new manifestations of ECD were present, including the following: a stellate appearance of intracranial extra-axial lesions, ependymal enhancement along the lateral ventricle with deep linear extension to the lentiform nucleus, irregular enhancement in the pons, and diffuse involvement of the vertebral column on PET/CT.

CONCLUSIONS: ECD has a variety of imaging appearances in the CNS, including new manifestations described herein. Neuroradiologists should be aware of these manifestations to avoid mistaking them for other disease processes.

ABBREVIATIONS: ECD = Erdheim-Chester disease; HPA = hypothalamic pituitary axis; SUV = standardized uptake value

First described in 1930, ECD is a rare non-Langerhans-cell histiocytosis, which typically affects patients in their fifth decade and more commonly affects men than women.[1,2] Pathologically, the disease is characterized by infiltration of tissues by lipid-laden histiocytes. The immunohistochemical profile differentiates this entity from the more common Langerhans type of histiocytosis.

Clinically, ECD can present in several forms; many patients are asymptomatic and are diagnosed with ECD when imaging is performed for other reasons.[3] Nonspecific bone pain is the most commonly reported symptom.[4] Radiographically, ECD can affect virtually any part of the body, but the most common site is bone, where it manifests as symmetric medullary sclerosis. There is a predilection for the appendicular skeleton, particularly the long bones of the upper and lower extremities. Other common sites of involvement include the perinephric soft tissues, retroperitoneum, mediastinum, and pulmonary interstitium.[5]

The clinical course varies widely, depending on the extent of disease, with some patients never developing symptoms and other patients succumbing after rapid disease progression.[2,6] Commonly reported causes of death in patients with ECD include renal failure, cardiomyopathy, and respiratory failure.[7]

Neurologic involvement is encountered in fewer than 50% of patients with proved ECD,[8] with the most common locations including the HPA, brain parenchyma, orbits, meninges, and paranasal sinuses. Less commonly affected areas include the spinal meninges and the bony spinal column.[8-10] When patients do have CNS involvement, they are often symptomatic, with diabetes insipidus and ataxia syndromes being the most common presentations.[5]

The purpose of this study was to review the findings on conventional imaging of the brain, head and neck, and spine in patients with ECD who presented to our institution and to identify atypical manifestations.

Materials and Methods

The institutional review board at the University of Texas MD Anderson Cancer Center approved this study and waived the requirement for informed consent. The clinical data and imaging studies for 11 patients who presented with ECD to our institution, a major cancer referral center, between August 1996 and July 2010, were retrospectively reviewed.

ECD was diagnosed either clinically or radiographically in all 11 patients. Additionally, pathologic confirmation was obtained in 10 of the 11 patients. The patient in whom pathologic confirmation was not available at our institution was diagnosed with and treated for ECD in Europe. She presented to our institution in septic shock and quickly succumbed to her acute process before she could be worked up and treated for ECD. The patients were screened for the presence of other chronic illnesses that may mimic ECD, including other histiocytic illnesses, leukemia, lymphoma, solid-organ malignancies, and sarcoidosis.

CT of the brain, neck, and spine was performed without and with administration of intravenous contrast material. MR imaging of the brain, orbits, and spine was performed on a 1.5T or 3T MR unit (GE Healthcare, Milwaukee, Wisconsin) and included T1 pre- and postcontrast, FLAIR, and fast spin-echo T2-weighted sequences; imaging was performed in at least 2 planes. A dedicated PET/CT system (Discovery ST, STE, or RX; GE Healthcare) was used to obtain images after intravenous administration of [^{18}F]FDG with a dose range of 9–19 mCi (mean, 12.1 mCi).

Received March 11, 2011; accepted after revision April 19, 2011.

From the Section of Neuroradiology (P.S., L.K., N.G.-T., J.M.D.), Departments of Radiology, Physics (P.H.), Pathology (M.D.W.), and Investigational Cancer Therapeutics (R.K.), University of Texas MD Anderson Cancer Center, Houston, Texas.

Please address correspondence to J. Mathew Debnam, MD, University of Texas MD Anderson Cancer Center, 1400 Pressler Blvd, Unit 1482, Houston, Texas 77030; e-mail: Matthew.Debnam@mdanderson.org

http://dx.doi.org/10.3174/ajnr.A2707

Patient demographics and imaging findings

No.	Age (yr)/ Sex	Symptoms	Areas of Involvement	Biopsy Sites	CNS Imaging Findings
1	37/F	Diffuse bone pain, extremity numbness, gait instability, diabetes insipidus	Pituitary/hypothalamus, brain stem, calvarium/skull base, spine, appendicular skeleton, lungs	Brain stem lesion, lung, left clavicle	Enlarged pituitary stalk, FLAIR hyperintensity hypothalamus, FLAIR hyperintensity/enhancement pons, lytic calvarial and mandibular lesions, spinal and sacral lesions (Fig 5)
2	69/M	Hydro-nephrosis	No CNS disease demonstrated, retroperitoneum, interstitial lung disease	Retroperitoneum, lung	NA
3	47/M	Hydro-nephrosis, diabetes insipidus	Pituitary, mediastinum, lung, retroperitoneum, appendicular skeleton	Renal	Enlarged pituitary stalk
4	66/M	Diabetes insipidus	Brain stem, sinuses, orbit, appendicular skeleton, retroperitoneum, renal	Sphenoid sinus, orbit, retroperitoneum, renal	T2 hyperintensity pons, sphenoid sinus mass, intraconal orbital mass, enlarged pituitary stalk
5	69/M	Diabetes insipidus	No CNS disease demonstrated, appendicular skeleton, retroperitoneum, chest	Femur, lung	NA
6	62/M	Numbness head and neck, gait instability	Brain stem, appendicular skeleton, perinephric infiltration	Tibia	FLAIR hyperintensity/enhancement pons and cerebellum (Fig 3)
7	61/F	Leg pain	No CNS disease demonstrated, appendicular skeleton, skin	Extremity soft tissues, tibia	NA
8	49/M	Fatigue, diabetes insipidus	Orbits, sella/cavernous sinuses, appendicular skeleton, retroperitoneum	Orbit	Intra-/extraonal orbital mass (Fig 4), sellar/cavernous sinus mass (Fig 4), enlarged pituitary stalk
9	60/M	Ascites	Calvarium/skull base, mesentery, retroperitoneum	Bone marrow	Enhancing calvarial foci
10	48/F	Fatigue, mental status change	Intracranial extra-axial, cerebellum, orbit, skull base	NA	IC extra-axial lesions (Fig 1), dentate nucleus hyperintensity, intraconal retrobulbar exophthalmos, sclerotic focus skull base
11	64/M	Abdominal pain, diabetes insipidus, extremity weakness	Intracranial, intra-axial, brain stem, cerebellum, orbit, mediastinum, retroperitoneum, appendicular skeleton	Pararenal	Ependymal enhancement to lentiform nucleus (Fig 2), FLAIR hyperintensity/enhancement, pons and cerebellum, intraconal orbital mass

Note:—NA indicates not applicable; IC, intracranial.

The studies were assessed for the presence of ECD in the following locations: the extra-axial and intra-axial intracranial compartments, HPA, cavernous sinus, orbits, skull, paranasal sinuses, and spine. When patients had coexisting illnesses that could have been mistaken for those with ECD, the records were carefully reviewed to determine whether the patients had ECD.

Results

Eleven patients (8 men, 3 women; 37–69 years of age; mean, 57.5 years; median, 61 years) were included in the study (Table). Of the 11 patients, 8 had CNS involvement, and all 11 presented with symptoms related to ECD, the most common being diabetes insipidus ($n = 6$). Eight patients did not have a history of another disease. Two patients had secondary disease, and 1, a developmental anomaly. The first patient, a 66-year-old man (patient 4), developed renal cell carcinoma, incidentally detected on cross-sectional imaging performed for the follow-up of ECD. This patient also had a history of hairy cell leukemia and was in remission when he presented with diabetes insipidus and retrobulbar mass lesions, diagnosed by biopsy as ECD. The second patient (patient 11) had a history of mucosa-associated lymphoid tissue lymphoma of the stomach, treated at another facility and in remission. He presented to our institution after biopsy of a sclerotic bone lesion revealed ECD. The final patient (patient 8) had imaging findings suggestive of septo-optic dysplasia (de Morsier syndrome), discovered after the diagnosis of ECD.

Supratentorial Extra-Axial Lesions

One (9%) patient (patient 10) had supratentorial extra-axial involvement. The patient was a 48-year-old woman with 5 large extra-axial masses, which measured 4.1–10.3 cm in diameter. Relative to gray matter, these masses were predominately hypoattenuated on CT and isointense on T1- and T2-weighted MR imaging with marked enhancement following contrast administration. All of these lesions had a stellate appearance (Fig 1), with spicules radiating from the center of each mass. These spicules were hyperattenuated on CT and hypointense on T1- and T2-weighted MR imaging and did not demonstrate enhancement.

Supratentorial Intra-Axial Lesion

One (9%) patient (patient 11) had supratentorial intra-axial involvement. The patient was a 64-year-old man whose imaging studies revealed curvilinear enhancement along the ependymal surface of the right lateral ventricle with linear extension into the right lentiform nucleus (Fig 2). There was associated FLAIR hyperintensity of this focus.

Fig 1. A 48-year-old woman (patient 10) who presented with fatigue and mental status change. Axial T1-weighted postgadolinium image of a bilateral parasagittal extra-axial mass demonstrates a stellate appearance, without enhancement of the spicules (*arrows*).

Infratentorial Intra-Axial Lesions

Five (45%) patients (3 men, 2 women; 37–66 years of age; mean, 55 years) had infratentorial intra-axial involvement. Three patients (patients 1, 6, and 11) had involvement of the pons and brachium pontis, with 2 of these patients having further signal-intensity abnormality extending into the cerebellar hemispheres. In all 3 patients, the abnormality manifested as patchy FLAIR hyperintensity, which was diffuse with expansion of the pons and brachium pontis. Associated enhancement was irregular and oriented transversely along the pons (Fig 3); this enhancement was diffuse ($n = 2$) or nodular ($n = 1$), with a small component extending in a transverse fashion. All 3 patients were symptomatic, with either unilateral weakness secondary to involvement of the corticospinal tracts or ataxia as a result of cerebellar involvement.

Patient 4 had a different pattern of involvement with diffuse T2 hyperintensity in the pons without associated enhancement or mass effect and was asymptomatic. Imaging studies of the final patient (patient 10) revealed bilateral diffuse dentate FLAIR hyperintensity without enhancement. This patient presented to our institution in septic shock and, soon after, succumbed to her acute illness, so it was not possible to clinically determine whether this lesion was symptomatic.

Lesions of the HPA

Four (36%) patients (3 men, 1 woman; 37–66 years of age; mean, 50 years) exhibited involvement of the HPA. Postcontrast T1-weighted MR imaging revealed an enlarged pituitary stalk in 2 patients (patients 3 and 4) but no abnormality in the pituitary gland itself. In another patient (patient 1), MR imaging demonstrated enhancement of pituitary stalk and FLAIR hyperintensity within the hypothalamus. Patient 8 had, in addition to disease in the sella turcica, extension into the bilateral cavernous sinuses (Fig 4). All 4 patients had symptoms related to diabetes insipidus.

Lesions of the Cavernous Sinus

One (9%) patient (patient 8) had involvement of the cavernous sinuses. The patient was a 49-year-old man who had enhancing soft-tissue masses in the sella, which extended laterally into the bilateral cavernous sinuses and encased the cavernous carotid arteries (Fig 4). There was no secondary imaging evidence of cavernous sinus occlusion, such as dilation of the superior ophthalmic vein or exophthalmos.

Lesions of the Orbits

Three (27%) patients (2 men, 1 woman; 48–66 years of age; mean, 54.3 years) had bilateral orbital involvement, with enhancing retrobulbar soft-tissue infiltration, which was hypointense on both T1- and T2-weighted images. All 3 patients had intraconal involvement. Patient 8 exhibited extraconal extension of disease (Fig 4), and patient 10 demonstrated exophthalmos.

Lesions of the Calvaria and Maxillofacial Bones

Three (27%) patients (2 women, 1 man; 37–60 years of age; mean, 48 years) had involvement of the calvaria or maxillofa-

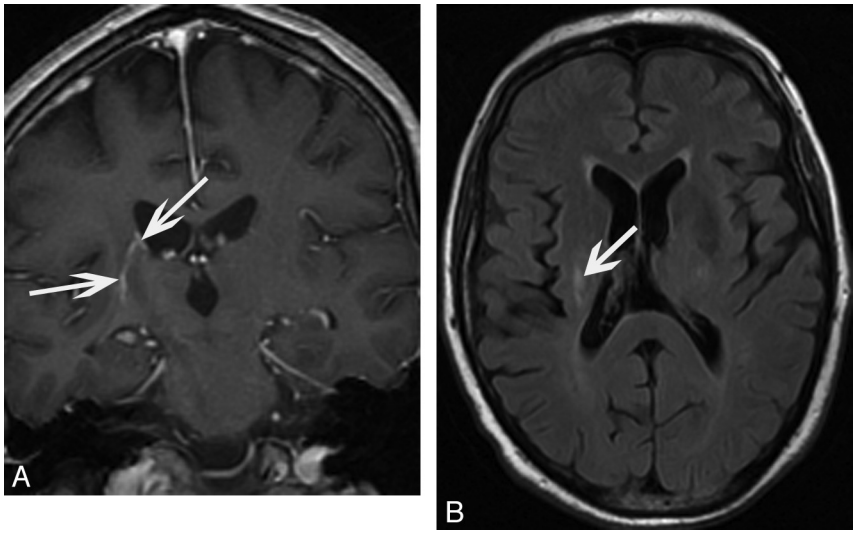

Fig 2. A 64-year-old man (patient 11) who presented with diabetes insipidus. *A,* Coronal T1-weighted postgadolinium image of an ependymal enhancing focus extending inferiorly toward the right lentiform nucleus (*arrows*). *B,* Axial FLAIR image demonstrates corresponding FLAIR signal-intensity hyperintensity (*arrow*).

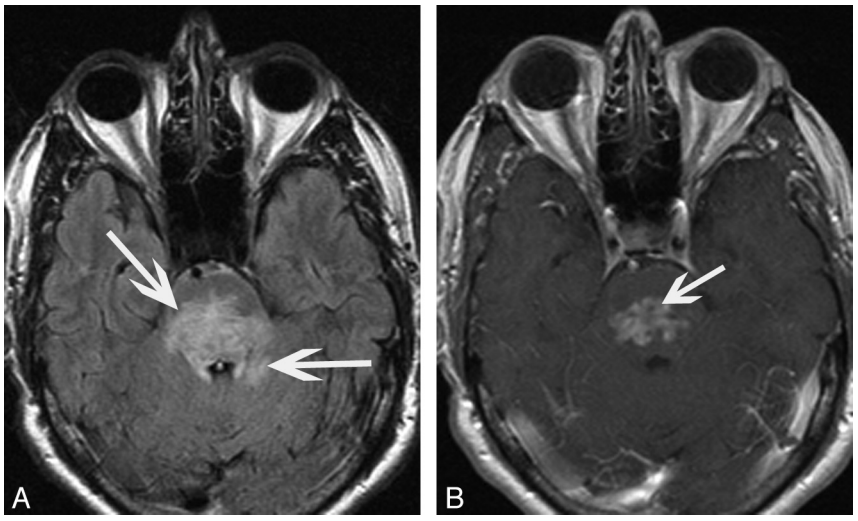

Fig 3. A 62-year-old man (patient 6) who presented with ataxia. *A,* Axial FLAIR image demonstrates hyperintensity in the pons with extension into the adjacent cerebellum (*arrows*). *B,* Axial T1-weighted postgadolinium image shows irregular heterogeneous enhancement oriented transversely along the pons (*arrow*).

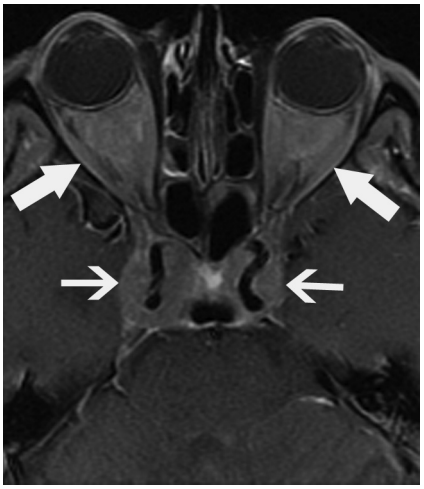

Fig 4. A 49-year-old man (patient 8) who presented with diabetes insipidus and fatigue. Axial T1-weighted postgadolinium image shows sellar and cavernous sinus involvement surrounding the cavernous carotid arteries (*small arrows*). Intra- and extraconal orbital involvement is also present (*large arrows*).

cial bones. In patient 9, MR imaging revealed diffuse heterogeneous signal intensity throughout the calvaria with faint enhancement; this patient did not have a corresponding CT scan. Patient 1 had a CT scan that revealed multiple lytic lesions in the mandible and calvaria, and MR imaging revealed corresponding T2-weighted hyperintense lesions. In the final patient (patient 10), a head CT revealed a sclerotic focus in the left skull base, which was not visualized on MR imaging.

Lesions of the Paranasal Sinuses

Involvement was identified in 1 (9%) patient (patient 4). The patient was a 66-year-old man who had opacification of the posterior ethmoid air cells and sphenoid sinuses without evidence of sinus expansion or bony sclerosis. On MR imaging, there was heterogeneous enhancement and T2 hypointense signal intensity identified in the sinus mass.

Lesions of the Vertebral Column

One (9%) patient (patient 1) had involvement of the bony spine on MR imaging. The patient was a 37-year-old woman whose MR imaging demonstrated diffuse marrow enhancing foci, corresponding to diffuse FDG avidity (Fig 5) on PET/CT.

Discussion

We report 4 new imaging appearances of ECD, including the following: a stellate appearance of intracranial extra-axial lesions, ependymal enhancement along the lateral ventricle with deep linear extension to the lentiform nucleus, irregular enhancement oriented transversely across the pons, and diffuse involvement of the vertebral column on PET/CT. The first new finding was that of an extra-axial lesion with radiating T2 hypointense spicules emanating from the center of the mass, without enhancement. A report by Caparros-Lefebvre et al[11] described 2 enhancing extra-axial lesions, 1 involving the frontal dura and the other, the falx, but without the pattern of spicules extending from the center of the mass. Other reports of patterns of extra-axial involvement have only described diffuse dural thickening and solitary "meningioma-like" masses[5,12,13] but have not reported this finding.

The second novel manifestation of ECD was ependymal enhancement along the lateral ventricle with linear extension inferiorly into the lentiform nucleus. Previous reports have described the presence of focal intra-axial mass lesions of the white matter and basal ganglia[12,14,15] but not this ependymal or linear enhancement. Several targeted treatments, including interferon and imatinib, have recently shown efficacy in ECD.[16-18] After treatment with interferon, follow-up imaging showed that the degree of enhancement in this lesion had decreased.

Involvement of the brain stem was present in 4 patients. Three of these patients demonstrated an enhancement pattern that was irregular and oriented transversely along the pons. This is different from the nodular pattern described in other reports.[2,5,12] This finding is also in contradistinction to the focal mass lesions reported in the supratentorial compartment.[12,14,15,19,20] The final patient demonstrated diffuse

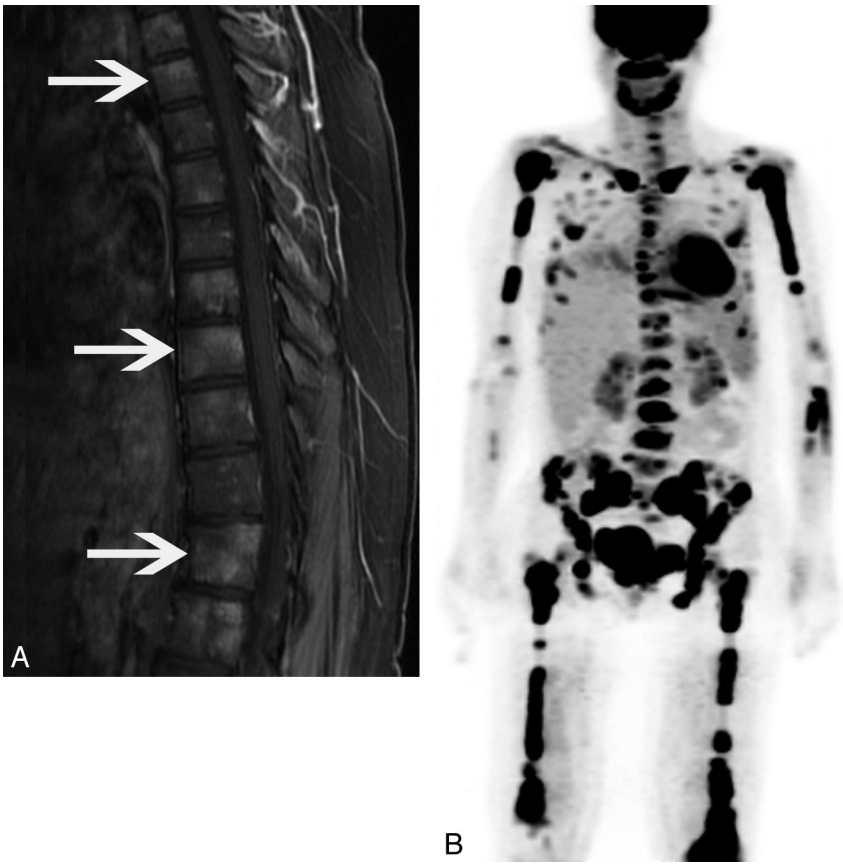

Fig 5. A 37-year-old woman (patient 1) who presented with gait instability. *A*, Sagittal T1-weighted postgadolinium image shows heterogeneously enhancing foci throughout the vertebral column (*arrows*). *B*, 3D PET further demonstrates diffuse FDG avidity in the spine, appendicular skeleton, and mandible.

FLAIR signal-intensity hyperintensity, similar to findings in a previous report by Bianco et al.[21]

HPA involvement has been reported as a single micronodular or nodular infundibular stalk mass[5] or thickening of the pituitary stalk.[12] This is similar to the findings in 3 patients in our study who demonstrated linear thickening of the pituitary stalk. In the fourth patient, the disease involved the sella and extended into the cavernous sinuses. Johnson et al[13] described a similar finding, with a sellar mass extending laterally into the cavernous sinus with encasement of the internal carotid arteries and extending posteriorly to encase the basilar artery. Drier et al[5] described pericarotid infiltration of the cervical segment of the internal carotid arteries, with intracranial extension into the cavernous sinuses.

One patient demonstrated diffuse involvement of the axial skeleton and sacrum on MR imaging with corresponding FDG avidity on PET/CT. Although bony spinal and canal involvement has been reported as a rare manifestation of ECD[9,11] and a case report discussed FDG avidity in a single vertebra,[8] to our knowledge, this is the first description of diffuse FDG avidity involving the axial skeleton.

Most of the patients in our study (8 of 11) had CNS involvement, a finding similar to that in a prior report by Drier et al,[5] who described CNS involvement in 30 of 33 patients. Three patients had orbital involvement, all within the intraconal space, a manifestation that has been described before,[5,11,22-24] and 1 had extension into the extraconal space, similar to findings in other reports.[5,23] One of the patients with orbital involvement had exophthalmos, which, along with vision loss, has been previously reported as a complication from

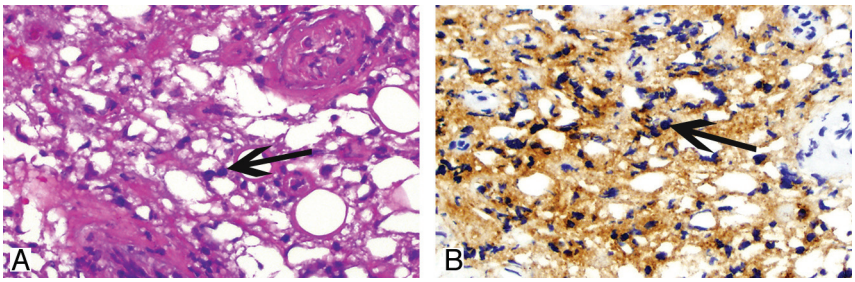

Fig 6. A 49-year-old man (patient 8, also described in Fig 4) with retro-orbital lesions. *A*, The orbital soft tissue is cellular with infiltration by predominance of foamy histiocytes (*arrow*) (hematoxylin-eosin, original magnification ×200). *B*, The cells are positive for CD68 (KP-1), consistent with histocytic origin (*arrows*) (CD68 immunohistochemical study, original magnification ×200). The cellular infiltrate is notably negative for CD1a on the CD1a immunohistochemical study (not shown).

orbital involvement.[22] Abnormal skull or maxillofacial involvement found in 3 (27%) of our patients is lower in frequency (80%) than that reported by Drier et al.[5] This difference may be due to the low number of patients in our study.

Our study does have a few limitations. It was a retrospective study with a relatively small patient population, and 10 of our 11 patients had biopsy-proved disease reviewed by our own pathologists. In addition, not every imaging technique was performed in each patient, due to the retrospective nature of the study. Another potentially limiting factor in our study was the fact that 2 of our patients had coexisting illnesses that might have been misinterpreted as ECD. However, after careful review of the coexistent illnesses and the time course and confirmatory pathologic biopsy, it became apparent that the imaging findings were, in fact, secondary to ECD and not the coexisting conditions.

On pathologic review, a hallmark of tissue involvement by ECD is an infiltration of large histiocytes with clear foamy cytoplasm (xanthoma cells) with a background of fibrosis (Fig 6). Chronic inflammation is also present, consisting of lymphocytes and plasma cells. Scattered Touton-type giant cells may also be identified. Further evaluation of the cellular infiltrate by immunohistochemical evaluation shows that the histiocytes are positive for expression of CD68 (KP-1), a histocytic marker, and variable for expression of S100. CD1a is notably negative in ECD histiocytes and, if present, would suggest Langerhans cell histiocytosis.

Conclusions

ECD has a variety of imaging appearances in the CNS. Four new manifestations of the disease include a stellate appearance of intracranial extra-axial lesions, ependymal enhancement along the lateral ventricle with deep linear extension, irregular enhancement oriented transversely across the pons, and diffuse involvement of the vertebral column on PET/CT. Neuroradiologists should be aware of these manifestations of ECD and consider the disease in the differential diagnosis when these findings are encountered.

Acknowledgments

We thank Markeda Wade for assistance in the preparation of this manuscript.

References

1. Veyssier-Belot C, Cacoub P, Caparros-Lefebvre D, et al. **Erdheim-Chester disease: clinical and radiologic characteristics of 59 cases.** *Medicine* 1996;75:157–69
2. Martinez R. **Erdheim-Chester disease: MR of intraaxial and extraaxial brain stem lesions.** *AJNR Am J Neuroradiol* 1995;16:1787–90
3. Bohlega S, Alwatban J, Tulbah A, et al. **Cerebral manifestation of Erdheim-Chester disease: clinical and radiologic findings.** *Neurology* 1997;49:1702–05
4. Gottlieb R, Chen A. **MR findings of Erdheim-Chester disease.** *J Comput Assist Tomogr* 2002;26:257–61
5. Drier A, Haroche J, Savatovsky J, et al. **Cerebral, facial, and orbital involvement in Erdheim-Chester disease: CT and MR imaging findings.** *Radiology* 2010;255:586–94
6. Vanichaniramol N, Kingpetch K, Buranasupkajorn P, et al. **Erdheim-Chester disease.** *Intern Med* 2008;47:1633–34
7. Shields JA, Karcioglu ZA, Shields CL, et al. **Orbital and eyelid involvement with Erdheim-Chester disease: a report of two cases.** *Arch Ophthalmol* 1991;109:850–54
8. Adam Z, Balsíková K, Pour L. **Diabetes insipidus followed, after 4 years, with dysarthria and mild right-sided hemiparesis: the first clinical signs of Erdheim-Chester disease— description and depiction of a case with a review of information on the disease** [in Czech]. *Vnitr Lek* 2009;55:1173–88
9. Allmendinger AM, Krauthamer AV, Spektor V, et al. **Atypical spine involvement of Erdheim-Chester disease in an elderly male.** *J Neurosurg Spine* 2010;12:257–60
10. Albayram S, Kizilkilic O, Zulfikar Z, et al. **Spinal dural involvement in Erdheim-Chester disease: MRI findings.** *Neuroradiology* 2002;44:1004–07
11. Caparros-Lefebvre D, Pruvo JP, Rémy M, et al. **Neuroradiologic aspects of Chester-Erdheim disease.** *AJNR Am J Neuroradiol* 1995;16:735–40
12. Lachenal F, Cotton F, Desmurs-Clavel H, et al. **Neurological manifestations and neuroradiological presentation of Erdheim-Chester disease: report of 6 cases and systematic review of the literature.** *J Neurol* 2006;253:1267–77
13. Johnson M, Aulino J, Jagasia M, et al. **Erdheim-Chester disease mimicking multiple meningiomas syndrome.** *AJNR Am J Neuroradiol* 2004;25:134–37
14. Tashjian V, Doppenberg EM, Lyders E. **Diagnosis of Erdheim-Chester disease by using computerized tomography-guided stereotactic biopsy of a caudate lesion: case report.** *Neurosurgery* 2004;101:521–27
15. Lyders EM, Kaushik S, Perez-Berenguer J, et al. **Aggressive and atypical manifestations of Erdheim-Chester disease.** *Clin Rheumatol* 2003;22:464–66
16. Janku F, Amin HM, Yang D, et al. **Response of histiocytoses to imatinib mesylate: fire to ashes.** *J Clin Oncol* 2010;28:633–36
17. Braiteh F, Boxrud C, Esmaeli B, et al. **Successful treatment of Erdheim-Chester disease, a non-Langerhans-cell histiocytosis, with interferon-alpha.** *Blood* 2005;106:2992–94
18. Esmaeli B, Ahmadi A, Tang R, et al. **Interferon therapy for orbital infiltration secondary to Erdheim-Chester disease.** *Am J Ophthalmol* 2001;132:945–47
19. Rushing EJ, Bouffard JP, Neal CJ, et al. **Erdheim-Chester disease mimicking a primary brain tumor: case report**. *J Neurosurg* 2004;100:1115–18
20. Rushing EJ, Kaplan KJ, Mena H, et al. **Erdheim-Chester disease of the brain: cytological features and differential diagnosis of a challenging case.** *Diagn Cytopathol* 2004;31:420–22
21. Bianco F, Iacovelli E, Tinelli E, et al. **Characteristic brain MRI appearance of Erdheim-Chester disease.** *Neurology* 2009;73:2120–22
22. de Palma P, Ravalli L, Grisanti F, et al. **Bilateral orbital involvement in Erdheim-Chester disease.** *Orbit* 1998;17:97–105
23. De Abreu MR, Chung CB, Biswal S, et al. **Erdheim-Chester disease: MR imaging, anatomic, and histopathologic correlation of orbital involvement.** *AJNR Am J Neuroradiol* 2004;25:627–30
24. Johns TT, Citrin CM, Black J, et al. **CT evaluation of perineural orbital lesions: evaluation of the "tram-track" sign.** *AJNR Am J Neuroradiol* 1984;5:587–90